Revision of Vajiralongkorn Dam's Reservoir Characteristic Curves Using NDWI Derived from Landsat 8 Data

Yutthana Phankamolsil[1] and Ekasit Kositsakulchai[2*]

[1]*Environmental Engineering and Disaster Management Program, Mahidol University, Kanchanaburi Campus, Saiyok, Kanchanaburi 71150, Thailand*
[2]*Department of Irrigation Engineering, Faculty of Engineering at Kamphaeng Saen, Kasetsart University, Nakhon Pathom 73140, Thailand*

ARTICLE INFO

Received: 17 Aug 2019
Received in revised: 20 Oct 2019
Accepted: 6 Nov 2019
Published online: 6 Dec 2019
DOI: 10.32526/ennrj.18.2.2020.13

Keywords:
Reservoir/ Storage capacity curve/ Remote sensing/ Landsat/ NDWI

*** Corresponding author:**
E-mail: ekasit.k@ku.th

ABSTRACT

Reservoir characteristics are the essential information for water management planning and reservoir operation. Regular monitoring and assessment of the reservoir characteristics can reduce risks associated with the reservoir operation. This research assessed the reservoir characteristics (water surface, volume) of Vajiralongkorn Dam using remote sensing. Reservoir water surface was classified using the Normalized Difference Water Index (NDWI) derived from the Landsat 8 data, and validated using the streamline matching rate (SMR) and the streamline matching error (SME) techniques for shoreline accuracy assessment. The volume between two water levels was calculated using the prismatic equation. The storage capacity curve was constructed from the reservoir water level and cumulative volume. The accuracy of NDWI technique was satisfactory in identifying reservoir water surface with a good accuracy of shoreline delineation (SMR>95% and SME=11.7 m). The water surface has decreased on the average of 8.2 km^2 (2.8%) compared with the original data in 1980. The storage capacity has decreased 495.3 million m^3 (MCM) over 38 years from 1980 to 2018, an annual capacity loss of 13 MCM. Finally, sustainable service of the reservoir needs better knowledge of the effects of storage loss, the erosion and sediment-transport processes, and conservation measures.

1. INTRODUCTION

The Vajiralongkorn (VJK) dam, located in the western Thailand has a large and important water storage reservoir. The dam was constructed in 1980 across the Kwai Noi River. The crossed construction in a river inevitably effects the sediment transport and accumulation. For this reason, the change in the sediment transport system leads to sediment accumulation problems resulting in the reduction of storage capacity and lifespan of reservoir (Morris and Fan, 1998; Fan and Morris, 1992a; Fan and Morris, 1992b). The reservoir characteristics (surface area and storage) are vital parameters in reservoir operation. Over the long period of operation, the reservoir characteristics changed due to morphology and human activity effects, such as sedimentation, land-use change or reclamation (Cesare et al., 2001). Therefore, it is essential to regularly survey and assess the reservoir characteristic curves. However, the financial cost has a great influence on the frequency of reservoirs survey (MacPheson et al., 2011).

There are two approaches commonly used to conduct the revision of reservoir characteristic curves. The first approach is bathymetric survey (Ortt et al., 2000; Odhiambo and Boss, 2004; Su et al., 2008; Grin, 2014). It relies on measuring the actual depths of water in the reservoir to calculate volume, in addition to bed-mapping the reservoir. For example, MacPheson et al. (2011) conducted bathymetric and topographic surveys to determine the water storage capacity, and the loss of capacity owing to sedimentation in Loch Lomond reservoir in Santa Cruz County, California. Other researchers including Su et al. (2008), Grin (2014), and Odhiambo and Boss

Citation: Phankamolsil Y, Kositsakulchai E. Revision of Vajiralongkorn Dam's reservoir characteristic curves using NDWI derived from Landsat 8 Data. Environ. Nat. Resour. J. 2020;18(2):134-145. DOI: 10.32526/ennrj.18.2.2020.13

(2004) likewise employed this approach. However, the approach requires time-consuming measurements, and needs several survey lines for generating a bed map. The second approach is an indirect method, which relies on a remote sensing technique (Pandey et al., 2016; Cui et al., 2013; Jain et al., 2002). Peng et al. (2006) estimated a new reservoir storage curve of Fengman reservoir in China using remote sensing. The NDWI technique was used to extract water body from Landsat TM images and compared with the observed data. The result showed that reservoir storage curve estimation is reasonable and has relatively high precision. Foteh et al. (2018) revised the live storage capacity and the total loss of Jayskwadi reservoir capacity due to the sediment deposition in India using Landsat 8 OLI/TIRS satellite data. The previous studies demonstrated the potential of remote sensing technique in assessing the reservoir sedimentation and analyzing its spatio-temporal variation. One of the common data source was the Landsat image (Avisse et al., 2017; Du et al., 2014; Rodrigues et al., 2012; Gupta and Banerji, 1985), especially for estimating reservoir storage loss (Zhang et al., 2018; El-Shazli and Hoermann, 2016; Ran and Lu, 2012).

This research investigated the remote sensing method for assessing water surface and volume of VJK reservoir. The specific objectives were to identify the water surface of VJK reservoir using the NDWI derived from the Landsat 8 data, and to estimate the VJK storage loss using the revised storage capacity curve.

2. METHODOLOGY

The overall methodology comprised four steps (Figure 1). Landsat image acquisition and preprocessing, reservoir surface water extraction, shoreline accuracy assessment, and storage capacity estimation.

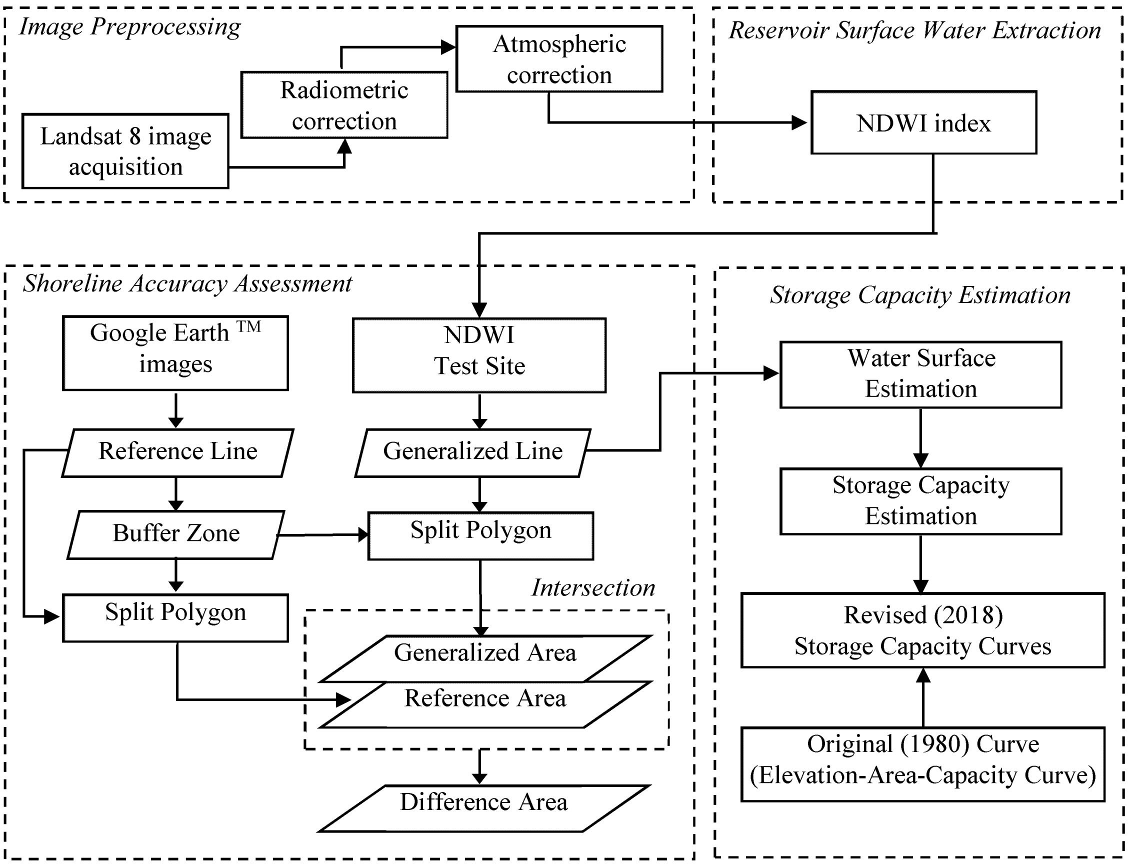

Figure 1. Overall methodology

2.1 Study site

The Vajiralongkorn (VJK) dam is located in Kanchanaburi province (about 150 km from the city center), in western Thailand (Figure 2). The dam is across the Kwai Noi River where the topography is mountainous. It is a rock-fill dam with a concrete facing slab that was constructed in 1980 and started operating in 1984. The reservoir was equipped to provide storage and release of water for multipurpose uses such as irrigation, flood control, hydropower generation, navigation, ecosystem, fishing and tourism. The reservoir has a surface area of 3,720 km^2 and length of 1.1 km; the height of the dam is 92 m above the river bed. The maximum pool level, the normal pool level, and the minimum pool level are respectively +160.5 m.a.s.l. (11,000 MCM), +155.0 m.a.s.l. (8,860 MCM), and +135.0 m.a.s.l. (3,012 MCM). The active storage is 5,848 MCM (difference between the normal and the minimum pool levels). Figure 2(e) shows the storage zones.

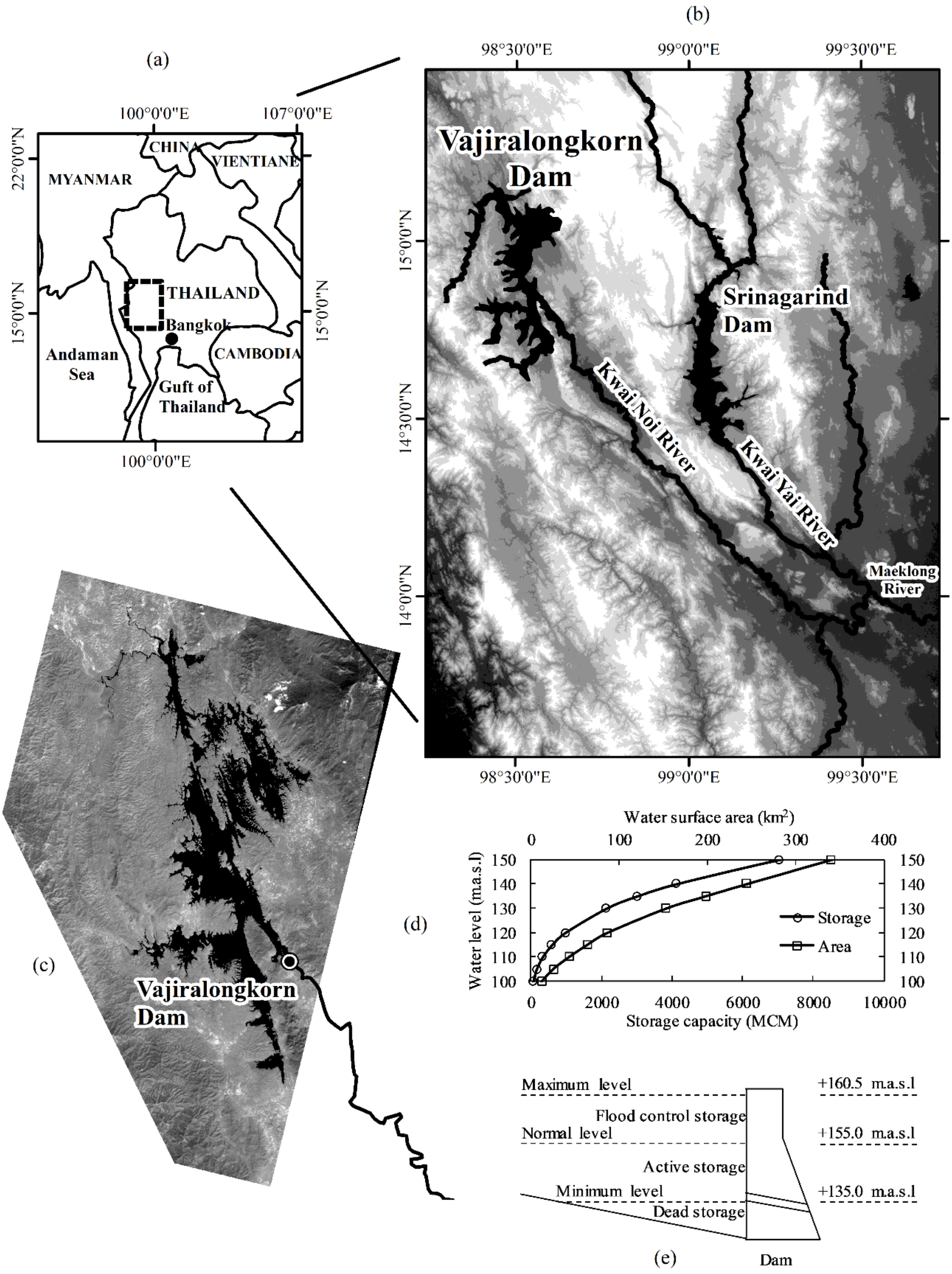

Figure 2. Location of the Vajiralongkorn (VJK) dam and reservoir characteristics: (a) regional map, (b) the Digital Elevation Model (DEM), (c) VJK reservoir from Landsat 8 false composite image, (d) VJK reservoir characteristic curves, and (e) VJK reservoir storage zoning.

2.2 Landsat 8 image

2.2.1 Data acquisition

The Landsat 8 satellite launched in February 2013, is the eighth American Earth observation (EO) satellite under the Landsat program, which is a collaboration between the National Aeronautics and Space Administration (NASA) and the United States Geological Survey (USGS). The Landsat 8 satellite collects the EO images with a 16-day repeat cycle (Scheffers and Kelletat, 2016). The Earth Explorer (http://earthexplorer.usgs.gov/) is the primary search interface for accessing images held in the USGS database. All images are distributed via Hypertext Transfer Protocol Secure (HTTPS), which are available to users at no cost. The image's data are stored in Geographic Tagged Image File Format (GeoTIFF) with Universal Transverse Mercator (UTM) projection and WGS84 datum. Twelve scenes (path 131, row 50) covering the entire VJK reservoir from 2013 to 2018 were selected (Table 1). The selection criteria were based on the range of reservoir water levels. Moreover, in order to avoid cloud disturbance, only the images with cloud cover less than 8% were selected.

2.2.2. Data pre-processing

Image pre-processing is an improvement of image data that maybe noisy or distorted during acquisition. The Landsat 8 OLI/TIRS images are acquired in the digital number (DN) format. Therefore, the radiometric calibration and atmospheric correction are prerequisite steps in order to generate the consistent and high-quality images, which consisted of three steps: (1) to convert DNs to the radiance based on the rescaling factors from the metadata file; (2) to convert radiance to TOA reflectance (Chander et al., 2009; Mishra et al., 2014), requiring additional information (Earth-Sun distance, solar zenith angle and exo-atmospheric irradiance); and (3) to apply atmospheric correction, requiring the atmospheric condition when the image was acquired. The atmospheric correction of Landsat images selected the Fast Line-of-Sight Atmospheric Analysis of Spectral Hypercubes (FLAASH) (Felde et al., 2003).

Table 1. Landsat 8 scene characteristics and the corresponding VJK reservoir water level

Acquisition date	Scene cloud cover (%)	Sun elevation L1 (degree)	Sun azimuth L1 (degree)	Reservoir water level (m.a.s.l.)
October 27th, 2013	1.06	56.1126559	142.6220	151.39
December 14th, 2013	1.53	46.0880237	148.7269	150.89
January 15th, 2014	0.10	45.72501243	142.9447	149.81
March 20th, 2014	7.65	59.88195648	116.8853	148.77
June 11th, 2015	2.70	64.98964157	66.1792	137.75
November 18th, 2015	1.39	51.20337824	147.3655	145.01
December 20th, 2015	2.01	45.40461047	147.7899	144.23
January 5th, 2016	0.24	44.97032311	145.1159	143.84
February 6th, 2016	0.14	48.80871324	136.1957	142.79
March 25th, 2016	2.40	61.14411182	113.2510	140.93
February 11th, 2018	0.86	49.98898489	134.2105	147.98
March 15th, 2018	3.37	58.39307113	119.6039	146.16

2.3 Estimation of reservoir characteristics

2.3.1 Reservoir surface water extraction

Reservoir shoreline was classified using the Normalized Difference Water Index (NDWI) (Deng et al., 2019; Ouma and Tateishi, 2007; Gao, 1996; McFeeters, 1996) which is a supervised classification technique applied for surface water detection with a selected suitable threshold. The NDWI designed to maximize reflectance of water by using the green wavelengths whereas water is reflected the lowest in the near-infrared band, opposite vegetation and soil which are the high reflections (Feyisa et al., 2014). The current research selected the threshold of zero to extract reservoir surface water. The NDWI is expressed as follows:

$$\text{NDWI} = \frac{\text{Green} - \text{NIR}}{\text{Green} + \text{NIR}} \tag{1}$$

Where, Green is the green wavelengths (Band 3 of Landsat 8 OLI), NIR is the near-infrared band (Band 5 of Landsat 8 OLI).

2.3.2 Reservoir storage capacity estimation

The storage capacity was estimated using the prismatic equation (Equation 2) (Peng et al., 2006) that calculates from the incremental volume between any two-stage elevations and the reservoir's active storage capacity:

$$V_{i+l} = \frac{(Z_{i+l} - Z_i)}{3} \left(A_i + A_{i+l} + \sqrt{A_i \times A_{i+l}}\right) \qquad (2)$$

Where, A_i and A_{i+l} are the reservoir water surface area at elevation Z_i and Z_{i+l} respectively, and V_{i+l} is the reservoir storage volume between Z_i and Z_{i+l} elevations. The storage capacity can calculate by the volume accumulation.

2.4 Accuracy assessment

2.4.1 Reference shoreline data

The high resolution images from Google Earth database were employed as the reference data for shoreline accuracy assessment. For this reason, the water surface data were not recorded by the observation data in the database of the Electricity Generating Authority of Thailand (EGAT) due to the large Vajiralongkorn dam and the water level fluctuation causing the change in water surface over time. Therefore, it is difficult to obtain the accurate ground-truth reservoir shoreline. The advantage of using Google Earth imagery is that it provides the latest imagery with high spatial resolution depending on the geographic viewed area. The reservoir shoreline can be visually seen on the image. Moreover, it provided images taken at different time periods which will be very useful for the researchers to perform the land cover change detection studies (Malarvizhi et al., 2016). However, the limitation of Google Earth imagery is that it is not possible to obtain the original multispectral band data (USGS, 2016), hence further image processing such as classification using unsupervised or supervised techniques is impracticable.

In the current study, the five sample sites (A1, A2, A3 A4, A5) surrounding the VJK reservoir were chosen for shoreline accuracy assessment by comparing the results between NDWI and Google Earth data (Figure 3). The sites were chosen based on the acquisition date of Google Earth history imagery which closely matched to the Landsat image scenes. In addition, it can represent the land cover characteristics on reservoir shoreline. It is not possible to compare the entire Vajiralongkorn shoreline since both image sources are different in acquisition time and scene size. The single Landsat scene is larger than the Google Earth image that was created using the satellite image mosaic. The Landsat acquisition information and Google Earth imagery are shown in Table 2.

2.4.2 Shoreline accuracy assessment

There are two steps in shoreline accuracy assessment: overlay analysis and streamline matching. The overlay analysis is a spatial analysis technique in GIS software**.** The on-screen digitizing and geo-referencing techniques were used for reference lines identification from the Google Earth imagery in the UTM/WGS84/zone47N projection system. Then, the buffer zone was created using the reference line offset of 30 m for error assessment; the offset distance is equal to the Landsat pixel resolution. The buffer zone was split into two sides as the "reference area". Secondly, the generalized line representing the reservoir shoreline was identified from the NDWI derived from the Landsat image. All image in raster data format was converted to vector data format using vectorization function. The buffer zone from the previous step was split using the generalized line as the "generalized area". Finally, the reference and generalized areas were overlay using the intersection function, which results in the difference area for calculating the streamline matching techniques.

The streamline matching techniques (Chen et al., 2012; Zhou, and Chen, 2011) compare the difference feature lines between the reference and generalized area (Figure 4). This approach can be divided by the streamline matching rate (SMR) and streamline matching error (SME). The SMR measures the changes rate in the length of generalized line or the shapes similarity between the reference and generalized line (Equation 3), while the SME calculates the average dispersion between the features (Equation 4):

$$\text{SMR} = \frac{L'}{L} \times 100 \qquad (3)$$

$$\text{SME} = \frac{\Delta A}{L} \times 100 \qquad (4)$$

Where, L is the total length of reference line, L′ is the length of generalized line within the buffer zone, and ΔA is the difference area between the reference line and generalized line within the buffer zone.

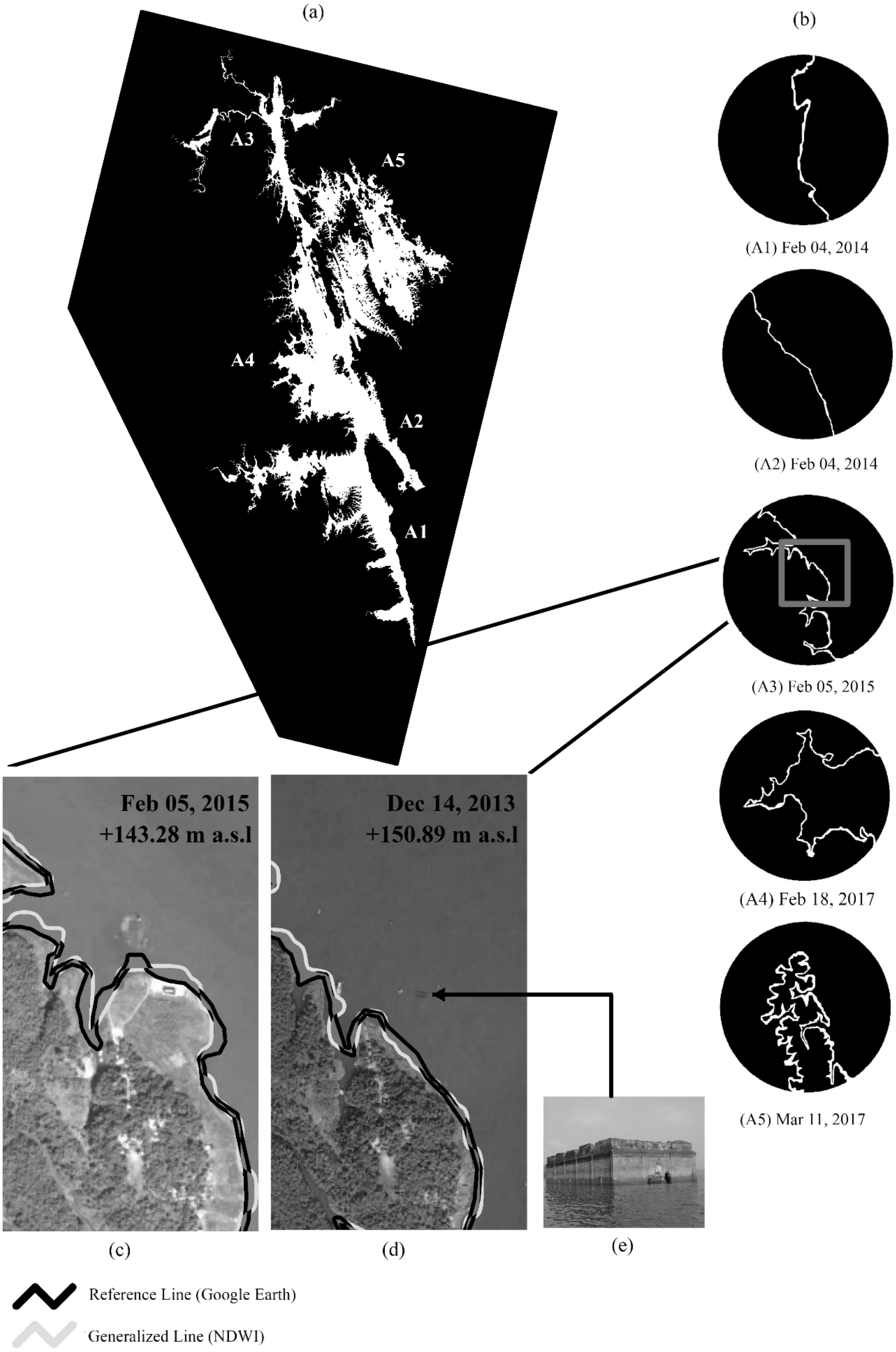

Figure 3. The shoreline sampling from high resolution images (Google Earth) as the reference lines for comparing with those derived from Landsat 8 data: (a) examples of shoreline extracted from the Google Earth high resolution images; (b) five sample locations surrounding the VJK Reservoir; (c) and (d), the sample location A3 on 5 February 2015 (c) and on 14 December 2013 (d) when reservoir water levels were respectively +143.28 m.a.s.l. and +150.89 m.a.s.l.; (e) the sunken temple as a reference location.

Table 2. Image acquisition dates of Landsat 8 scenes and Google Earth high resolution images and the corresponding VJK reservoir's water level

Location	Landsat scene		Google Earth Image	
	Date	Water level (m.a.s.l.)	Date	Water level (m.a.s.l.)
A1	Feb 09, 2014	148.28	Feb 09, 2014	148.28
	Mar 12, 2017	143.21	Mar 11, 2017	143.21
A2	Feb 09, 2014	148.28	Feb 02, 2014	148.72
	Mar 12, 2017	143.17	Mar 11, 2017	143.21
A3	Dec 14, 2013	150.89	Dec 14, 2013	150.89
	Feb 03, 2015	150.89	Feb 05, 2015	143.28
A4	Feb 09, 2014	150.89	Dec 14, 2013	150.89
	Feb 08, 2017	144.13	Dec 14, 2013	144.13
A5	Feb 09, 2014	150.89	Dec 14, 2013	150.89
	Mar 12, 2017	143.36	Feb 05, 2015	143.31

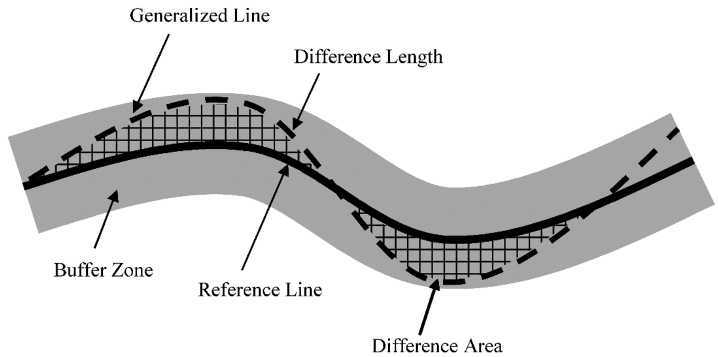

Figure 4. The streamline matching techniques: the reference line is the reservoir's shoreline that was digitized from Google Earth map; the generalized line is the water surface line identified using NDWI; the buffer zone is the tolerance zone and the distance from the reference line; the difference length is the difference length of generalized line from the reference line within buffer zone; and difference zone denotes the area that are not compatible within the buffer zone.

3. RESULTS

3.1 Reservoir water surface

The water surface of VJK reservoir identified using NDWI derived from Landsat 8 is shown in Figure 5. The water surface area was clearly discerned from the bright pixels. Table 3 shows the comparison of the water surface area between the NDWI-derived area and the original area (1980) at the water level from +137.75 m.a.s.l. to +151.39 m.a.s.l. The water surface area expands with the increasing of reservoir water level. The original data in 1980 reported the largest area of 318.8 km^2 (+151.39 m.a.s.l.) and the smallest of 201.8 km^2 (+137.75 m.a.s.l.), while the revised data using NDWI technique were respectively 310.7 km^2 and 197.4 km^2. The scatter plot (Figure 6(a)) indicated high correlation between the original area (1980) and the NDWI techniques (r^2=0.9679). There was no trend in the residual plot (Figure 6(b)). The mean of difference between the revised area and the original one was -8.2 km^2 (-2.8%) and ranged between -0.2 km^2 (-0.1%) and -25.7 (-9.7%) (Table 3).

The accuracy of VJK Reservoir's shoreline identification was assessed using the SMR and SME. The comparison of the shoreline between the generalized lines (derived from NDWI) and the reference lines (from high resolution images) which selected from five locations surrounding the shoreline of VJK reservoir (Figure 3). The result of accuracy assessment is shown in Table 4. The mean of SMR was 95.1%; the SMR indicated the proportion of the length of generalized line within the buffer zone to the total length of reference line (Equation 3). The mean of SMR error was -4.9%, while the highest and the lowest SMR errors were respectively -12.1% and + 2.0%. The mean of SME was 11.7 m; the SME estimated from the ratio of the difference area between the reference line and generalized line to the total length of reference line (Equation 4). The highest and the lowest SME are respectively 17.9 m and 6.3 m. The values of SME were lower than the resolution (30 m) of Landsat image.

Table 3. Comparison of water surface area of VJK reservoir between the original data in 1980 and the revision one from NDWI technique

Water level (m.a.s.l.)	Reservoir water surface area (km^2)		Difference from the original	
	Original (1980)	NDWI	(km^2)	(%)
137.75	201.8	197.4	-4.5	2.2
140.93	229.0	227.2	-1.8	0.8
142.79	244.9	239.2	-5.6	2.3
143.84	253.9	237.7	-16.2	6.4
144.54	259.9	247.2	-12.7	4.9
145.01	263.9	238.2	-25.7	9.7
146.16	273.8	273.6	-0.2	0.1
147.98	289.4	286.2	-3.2	1.1
148.77	296.2	295.2	-1.0	0.3
149.81	305.2	300.5	-4.7	1.5
150.89	314.5	299.5	-15.0	4.8
151.39	318.8	310.7	-8.1	2.5
Average			-8.2	2.8

Table 4. Accuracy assessment of shoreline of VJK reservoir derived from NDWI

Sample site	Acquisition date	ΔA (m^2)	L (m)	L′ (m)	SMR (%)	SMR error (%)	SME (m)
A1	Feb 09, 2014	55,920	3,135	3,240	103.3	+3.3	17.8
	Mar 12, 2017	51,399	2,882	2,942	102.0	+2.0	17.9
A2	Feb 09, 2014	15,562	2,590	2,489	96.1	-3.9	6.3
	Mar 12, 2017	17,058	2,589	2,480	95.8	-4.2	6.9
A3	Dec 14, 2013	62,402	7,601	7,155	94.1	-5.9	8.3
	Feb 03, 2015	61,043	8,032	7,060	87.9	-12.1	7.6
A4	Feb 09, 2014	147,417	8,638	7,938	91.9	-8.1	17.1
	Feb 08, 2017	77,136	8,177	7,667	93.8	-6.2	9.4
A5	Feb 09, 2014	129,374	12,265	10,802	97.8	-2.2	10.5
	Mar 12, 2017	194,786	12,242	10,808	88.3	-11.7	15.9
				Mean	95.1	-4.9	11.7

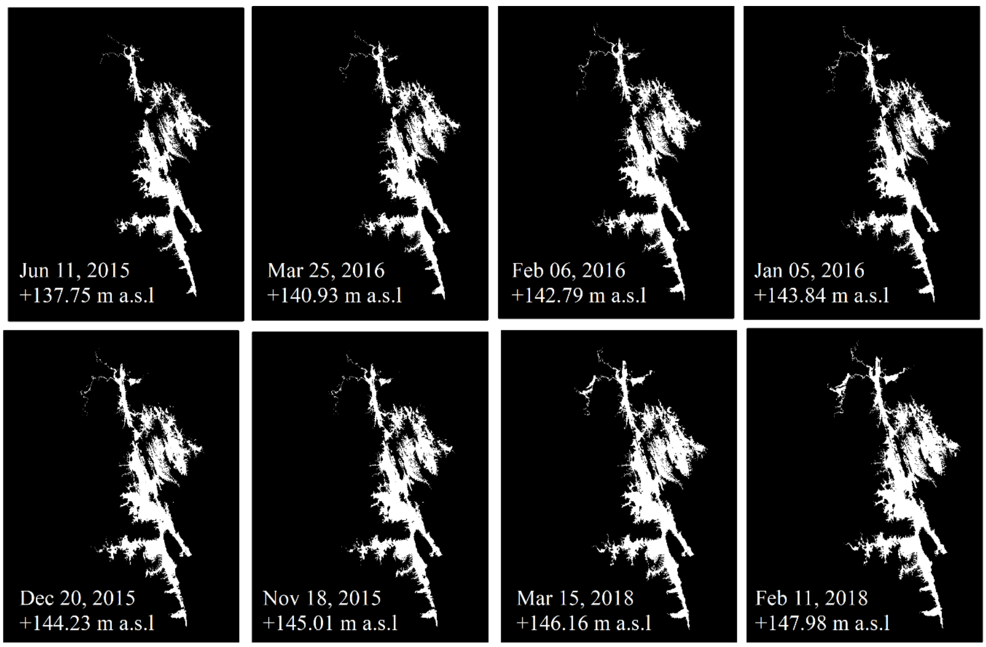

Figure 5. Water surfaces of VJK reservoir from water level of +137.75 m.a.s.l. to 151.39 m.a.s.l. identified using NDWI derived from Landsat 8 data

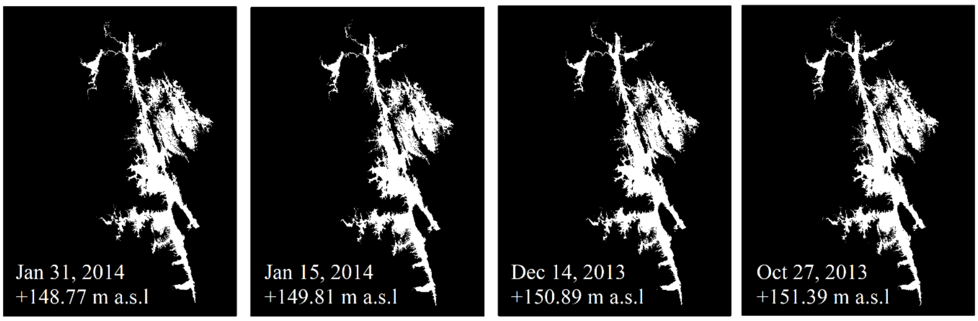

Figure 5. Water surfaces of VJK reservoir from water level of +137.75 m.a.s.l. to 151.39 m.a.s.l. identified using NDWI derived from Landsat 8 data (cont.)

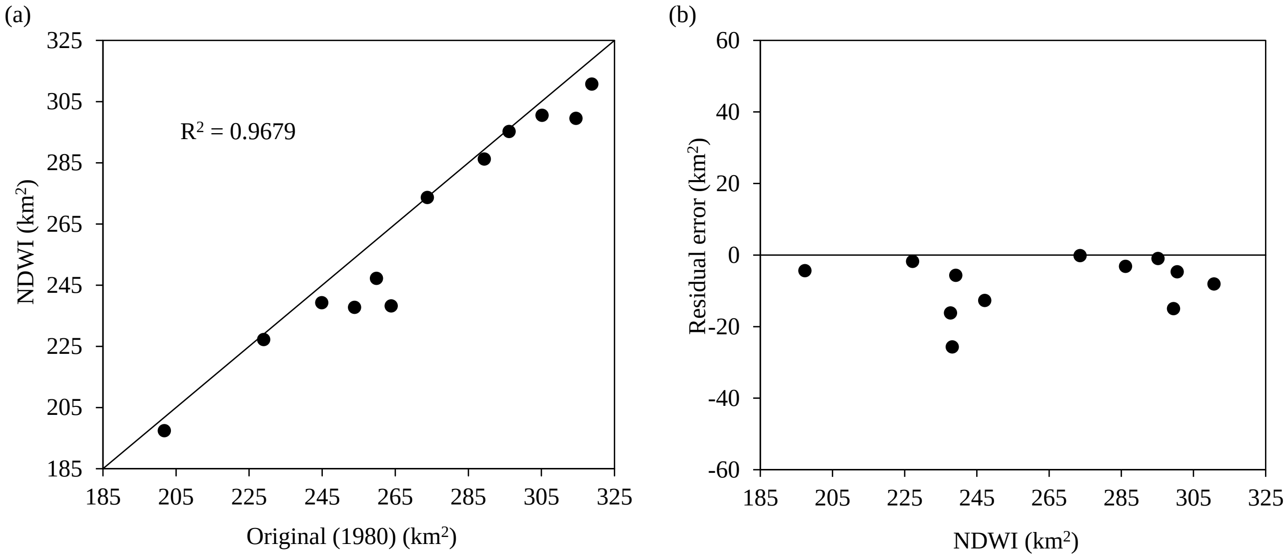

Figure 6. Comparison of the water surface areas of VJK reservoir between the original data in 1980 and the revised one using NDWI technique: (a) Scatter plot, (b) Residual errors

3.2 Reservoir storage capacity curve

The storage capacity curve was derived from the accumulated volume calculated using the prismatic equation (Equation 2). Table 5 and Figure 7 show the comparison of the reservoir storage capacity between the original curve (1980) and the revised curve (2018) at the water level from +137.75 m.a.s.l. to +151.39 m.a.s.l. The initial storage (3,006.4 MCM) was set at the minimum water level (+135.00 m.a.s.l.). The storage capacity of the revised curve arrived the maximum volume of 7,030.2 MCM at water level +151.39 m.a.s.l. Figure 7 show the comparison of cumulative curves between the original curve (1980) and revised one (2018): water level and water surface areas (Figure 7(a)), and water level and storage capacity (Figure 7(b)). The storage capacity of VJK reservoir was decreased 495.3 MCM (6.6 %) at the water level +151.39 m.a.s.l. The annual capacity loss from 1980 to 2018 was estimated at 13 MCM.

Table 5. Comparison of reservoir characteristics (water surface and volume) of the Vajiralongkorn Dam between the original data in 1980 and the revision in 2018

Water level (m.a.s.l.)	Level difference (m)	Water surface (km^2)		Incremented volume (MCM)		Cumulative volume (MCM)		Difference from original	
		Original (1980)	Revised (2018)	Original (1980)	Revised (2018)	Original (1980)	Revised (2018)	(MCM)	(%)
135.00	0.0	178.4	177.8	0.0	0.0	3,006.4	3,006.4	0.0	0.0%
137.75	2.8	201.8	197.4	581.1	525.0	3,587.5	3,531.4	-56.1	-1.6%
140.93	3.2	229.0	227.2	761.0	678.8	4,348.5	4,210.2	-138.3	-3.2%
142.79	1.9	244.9	239.2	489.4	443.0	4,837.9	4,653.3	-184.6	-3.8%
143.84	1.1	253.9	237.7	290.7	262.3	5,128.6	4,915.6	-213.0	-4.2%

Table 5. Comparison of reservoir characteristics (water surface and volume) of the Vajiralongkorn Dam between the original data in 1980 and the revision in 2018 (cont.)

Water level (m.a.s.l.)	Level difference (m)	Water surface (km^2)		Incremented volume (MCM)		Cumulative volume (MCM)		Difference from original	
		Original (1980)	Revised (2018)	Original (1980)	Revised (2018)	Original (1980)	Revised (2018)	(MCM)	(%)
144.54	0.7	259.9	247.2	199.6	169.7	5,328.2	5,085.3	-242.9	-4.6%
145.01	0.5	263.9	238.2	136.6	121.3	5,464.8	5,206.6	-258.2	-4.7%
146.16	1.2	273.8	273.6	343.0	306.8	5,807.8	5,513.5	-294.3	-5.1%
147.98	1.8	289.4	286.2	568.4	503.8	6,376.2	6,017.2	-359.0	-5.6%
148.77	0.8	296.2	295.2	256.5	232.6	6,632.7	6,249.8	-382.9	-5.8%
149.81	1.0	305.2	300.5	346.6	297.8	6,979.3	6,547.6	-431.7	-6.2%
150.89	1.1	314.5	299.5	370.8	330.0	7,350.1	6,877.6	-472.5	-6.4%
151.39	0.5	318.8	310.7	175.4	152.5	7,525.5	7,030.2	-495.3	-6.6%

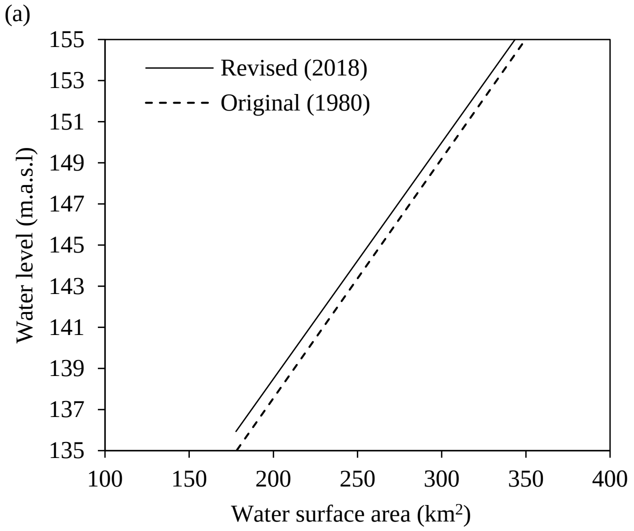

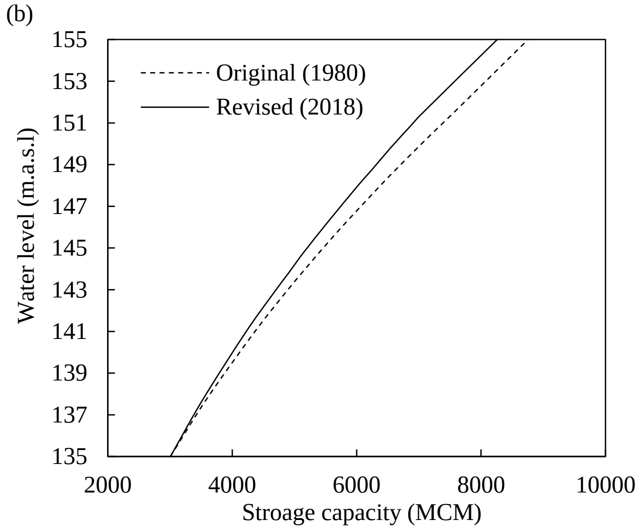

Figure 7. Comparison between original (1980) and revised (2018) reservoir characteristic curves of Vajiralongkorn Dam, (a) water level vs water surface area curve, (b) water level vs storage capacity curve

4. DISCUSSION AND CONCLUSION

The water surface area of VJK reservoir decreased on the average of 8.2 km^2 comparing with the original data in 1980, which is consistent with the reports in other studies. For example, El-Shazli and Hoermann (2016), Jeyakanthan and Sanjeevi (2011) and Fan and Morris (1992b) reported that the morphology of reservoir had changed because of sedimentation.

In conclusion, this paper investigated the assessment of water surface and volume of VJK reservoir using NDWI derived from Landsat 8 data. The accuracy of NDWI technique was satisfactory in identifying reservoir water surface. The water surface decreased on the average of -8.2 km^2 (-2.8%) comparing with the original data in 1980. The storage capacity of VJK reservoir was decreased 495.3 MCM over 38 years from 1980 to 2018 with the annual capacity loss of 13 MCM.

Remote sensing is an effective method in land and water monitoring. Landsat 8 provides a compromised option between spatial and temporal resolutions. Water surface and volume of VJK reservoir were successfully estimated using NDWI technique, however, only reservoir water levels ranged from +137.75 m.a.s.l. to 151.39 m.a.s.l. were monitored. The estimation of entire range of reservoir water level is an arduous task because it requires more satellite data. Cloud covering, especially during the rainy season makes satellite images inapplicable. In addition, the current research did not directly measured the sediment accumulation, but it is rather an indirect technique. Bathymetric survey is recommended for collecting reservoir bottom elevations particularly below the minimum water level of the VJK reservoir (+135 m.a.s.l.).

For further research, the evaluation of the effects of storage loss should be addressed both on the operation performance of the VJK dam and on the water resource management in the Mae Klong River Basin. The understanding on the erosion and sediment transport processes in the VJK watershed should be improved. Appropriate conservation measures should be studied and put into practice in the upstream forests of VJK dam.

ACKNOWLEDGEMENTS

The authors express their gratitude to the Electricity Generating Authority of Thailand (EGAT) for the Vajiralongkorn dam's data and to the USGS for Landsat 8 data from the website (http://earthexplorer.usgs.gov/). The software licenses in this study (ArcGIS and ENVI) were provided by the Faculty of Environment and Resource Studies, Mahidol University, Thailand.

REFERENCES

Avisse N, Tilmant A, Müller MF, Zhang H. Monitoring small reservoirs' storage with satellite remote sensing in inaccessible areas. Hydrology and Earth System Sciences 2017;21(12): 6445-59.

Cesare DD, Schleiss A, Hermann F. Impact of turbidity currents on reservoir sedimentation. Journal of Hydraulic Engineering 2001;127(1):6-16.

Chander G, Markham BL, Helder DL. Summary of current radiometric calibration coefficients for Landsat MSS, TM, ETM+, and EO-1 ALI sensors. Remote Sensing of Environment 2009;113(5):893-903.

Chen Y, Wilson J, Zhu Q, Zhou Q. Comparison of drainage-constrained methods for DEM generalization. Computers and Geosciences 2012;48:41-9.

Cui L, Qiu Y, Fei T, Liu Y, Wu G. Using remotely sensed suspended sediment concentration variation to improve management of Poyang Lake, China. Lake and Reservoir Management 2013;29(1):47-60.

Deng Z, Sun Y, Zhang K, Qiu Q, Sun W. A water identification method basing on grayscale Landsat 8 OLI images. Geocarto International 2019:1-11.

Du Z, Li W, Zhou D, Tian L, Ling F, Wang H, et al. Analysis of Landsat-8 OLI imagery for land surface water mapping. Remote Sensing Letters 2014;5(7):672-81.

El-Shazli A, Hoermann G. Development of storage capacity and morphology of the Aswan High Dam Reservoir. Hydrological Sciences Journal 2016;61(14):2639-48.

Fan J, Morris GL. Reservoir sedimentation. I: delta and density current deposits. Journal of Hydraulic Engineering 1992a; 118(3):354-69.

Fan J, Morris GL. Reservoir sedimentation. II: Reservoir desiltation and long-term storage capacity. Journal of Hydraulic Engineering 1992b;118(3):370-84.

Felde GW, Anderson GP, Cooley TW, Matthew MW, Adler-Golden SM, Berk A, et al. Analysis of hyperion data with the FLAASH atmospheric correction algorithm. Proceedings of the International Geoscience and Remote Sensing Symposium (IGARSS); 2003 Jul 21-25; Toulouse, France; 2003.

Feyisa GL, Meilby H, Fensholt R, Proud SR. Automated water extraction index: A new technique for surface water mapping using Landsat imagery. Remote Sensing of Environment 2014;140:23-35.

Foteh R, Garg V, Nikam BR, Khadatare MY, Aggarwal SP, Kumar AS. Reservoir sedimentation assessment through remote sensing and hydrological modelling. Journal of the Indian Society of Remote Sensing 2018;46(11):1893-905.

Gao B-C. NDWI-A normalized difference water index for remote sensing of vegetation liquid water from space. Remote Sensing of Environment 1996;58(3):257-66.

Grin S. Geometry and water height-area-volume curves of the reservoirs in the semiarid Madalena basin in Northeast Brazil [Bachelor final project]. Enschede, University of Twente; 2014.

Gupta RP, Banerji S. Monitoring of reservoir volume using LANDSAT data. Journal of Hydrology 1985;77(1):159-70.

Jain SK, Singh P, Seth SM. Assessment of sedimentation in Bhakra Reservoir in the western Himalayan region using remotely sensed data. Hydrological Sciences Journal 2002;47(2):203-12.

Jeyakanthan VS, Sanjeevi S. Reservoir capacity estimation of Singoor reservoir, India, by per-pixel and sub-pixel processing of multi-date satellite images. Geocarto International 2011;26(4):305-20.

MacPheson KR, Freeman LA, Flint LE. Analysis of Methods to Determine Storage Capacity of, and Sedimentation in, Loch Lomond Reservoir, Santa Cruz County, California, 2009. Reston, VA: U.S. Geological Survey; 2011.

Malarvizhi K, Kumar SV, Porchelvan P. Use of high resolution Google Earth satellite imagery in landuse map preparation for urban related applications. Procedia Technology 2016; 24:1835-42.

McFeeters SK. The use of the Normalized Difference Water Index (NDWI) in the delineation of open water features. International Journal of Remote Sensing 1996;17(7):1425-32.

Mishra N, Haque M, Leigh L, Aaron D, Helder D, Markham B. Radiometric cross calibration of Landsat 8 operational land imager (OLI) and Landsat 7 Enhanced Thematic Mapper Plus (ETM+). Remote Sensing 2014;6(12):12619-38.

Morris GL, Fan J. Reservoir Sedimentation Handbook: Design and Management of Dams, Reservoirs, and Watersheds for Sustainable Use. New York, USA: McGraw-Hill; 1998.

Odhiambo BK, Boss SK. Integrated echo sounder, GPS, and GIS for reservoir sedimentation studies: Examples from two Arkansas lakes. Journal of the American Water Resources Association 2004;40(4):981-97.

Ortt RA, Kerhin RT, Wells D, Cornwell J. Bathymetric Survey and Sedimentation Analysis of Loch Raven and Prettyboy Reservoirs. Coastal and Estuarine Geology File Report. Baltimore, MD: Maryland Geological Survey; 2000.

Ouma YO, Tateishi R. Lake water body mapping with multiresolution based image analysis from medium-resolution satellite imagery. International Journal of Environmental Studies 2007;64(3):357-79.

Pandey A, Chaube UC, Mishra SK, Kumar D. Assessment of reservoir sedimentation using remote sensing and recommendations for desilting Patratu Reservoir, India. Hydrological Sciences Journal 2016;61(4):711-8.

Peng D, Guo S, Liu P, Liu T. Reservoir storage curve estimation based on remote sensing data. Journal of Hydrologic Engineering 2006;11(2):165-72.

Ran L, Lu XX. Delineation of reservoirs using remote sensing and their storage estimate: an example of the Yellow river basin, China. Hydrological Processes 2012;26(8):1215-29.

Rodrigues LN, Sano EE, Steenhuis TS, Passo DP. Estimation of small reservoir storage capacities with remote sensing in the Brazilian Savannah region. Water Resources Management 2012;26(4):873-82.

Scheffers AM, Kelletat DH. Lakes of the World with Google Earth, Understanding Our Environment. Dordrecht, the Netherlands: Springer; 2016.

Su H, Liu H, Heyman WD. Automated derivation of bathymetric information from multi-spectral satellite imagery using a non-linear inversion model. Marine Geodesy 2008;31(4):281-98.

United States Geological Survey (USGS). Landsat 8 (L8) Data User's Handbook. Sioux Falls, SD: Earth Resources Observation and Science Center; 2016.

Wu C-H, Chen C-N, Tsai C-H, Tsai C-T. Estimating sediment deposition volume in a reservoir using the physiographic soil erosion-deposition model. International Journal of Sediment Research 2012;27(3):362-77.

Zhang F, Li J, Zhang B, Shen Q, Ye H, Wang S, et al. A simple automated dynamic threshold extraction method for the classification of large water bodies from landsat-8 OLI water index images. International Journal of Remote Sensing 2018;39(11):3429-51.

Zhou Q, Chen Y. Generalization of DEM for terrain analysis using a compound method. ISPRS Journal of Photogrammetry and Remote Sensing 2011;66(1):38-45.